Supporting Information

Constructing Mo-O-Ni anchoring bonds by room temperature solid-state reduction to drive hydrogen spillover for saturated hydrogenation of naphthalene

Guo Chen‡, Jinhua Wang‡, Tingting Cui, Yakun Tang, Yue Zhang, Ting Liu, Xiaodong Zhou, Xiaodong Guo and Lang Liu**

State Key Laboratory of Chemistry and Utilization of Carbon Based Energy Resources; Key Laboratory of Energy Materials Chemistry, Ministry of Education; College of Chemistry, Xinjiang University, Urumqi 830017, China

*Corresponding Authors: yktang@xju.edu.cn, liulang@xju.edu.cn.

Experimental Section

Materials

All chemicals were used without further purification. Sodium borohydride ($NaBH_4$, 99%) was obtained from Xilong Scientific Co., Ltd. Phosphomolybdic acid hydrate ($H_3Mo_{12}O_{40}P \cdot xH_2O$, 99%) was obtained from Sinopharm Chemical Reagent Co., Ltd. Nickel(II) chloride($NiCl_2 \cdot 6H_2O$, 98%), were obtained from Tianjin Xinbote Chemical Co., Ltd. Polyethylene glycol 400 (PEG-400) were purchased from Tianjin Guangfu Chemical Reagent Co., Ltd. Naphthalene ($C_{10}H_8$, 99%) was purchased from Shanghai Macklin Biochemical Technology Co., Ltd. Extraction solvents and N-hexane were analytical grade and purchased from Tianjin Zhiyuan Chemical Reagent Co, Ltd.

Preparation of catalysts

x%-PMA@Ni catalysts were prepared by the room temperature solid-state chemical reaction.[1,2] In a typical synthesis, $NiCl_2 \cdot 6H_2O$ (0.48g, 2 mmol) and $H_3\,PMo_{12}O_{40} \cdot xH_2O$ (PMA) with PMA-to-Ni mass ratios of x wt% (x = 0, 6, 12, 24) were placed in an agate mortar and manually ground for 10 min. Subsequently, 1 mL PEG-400 was added. The mixture was then ground for 5 min. Next, 2 mmol $NaBH_4$ was introduced in one portion and the mixture was ground again for 30 min until a uniform black powder was formed. The solid was washed with deionized water and ethanol to remove PEG-400 and by-products, then dried in vacuo at 60 °C for 6 h to yield the corresponding x%-PMA@Ni catalysts.

Characterization of catalysts

The crystal phases of the samples were characterized by XRD (Bruker D8) with a

Cu-K radiation source (λ = 1.54 Å). The morphology and structure were observed using scanning electron microscope (SEM, Hitachi SU4800) and transmission electron microscopy (TEM, Talos F200x). XPS (Thermo ESCALAB 250Xi) was used to examine the elemental distribution, analyze the elemental composition and determine bonding type. Fourier transform infrared spectroscopy (FT-IR) was performed on a VERTEX 70 RAMI Fourier transform IR (FTIR) spectrometer at room temperature. Pyridine adsorption infrared spectroscopy (Py-FTIR) was carried out on a Thermo Fisher Nicolet iS50 spectrometer for detecting accessible surface acidic sites, recording 1700-1400 cm^{-1}.

Test of catalysts on a model compound

First, 0.10 g model compound (Naphthalene), 20 mL *n*-hexane and 0.05 g catalyst were added into a 100 mL stainless steel autoclave. The air in the autoclave was exchanged with N_2 for 3 times and pressurized with 0.5-2.0 MPa H_2 at room temperature. Afterwards, the reactor was heated to a desired temperature and held at that temperature for some time. Finally, the reactor was cooled to room temperature, and the reaction mixture was filtered. The filtrate was analyzed by gas chromatography/mass spectrometer (GC/MS). Dodecane was used as an internal standard to quantify the products. Each experiment was repeated at least three times to ensure the repeatability of the data.

$$\text{Conversion}\ (\%) = \frac{\text{moles of substrate reacted}}{\text{moles of substrate supplied}} \times 100\%$$

$$\text{Selectivity}\ (\%) = \frac{\text{moles of each component}}{\text{moles of substrate reacted}} \times 100\%$$

Computational Method

All calculations were performed using density functional theory (DFT) within the Vienna ab-initio Simulation Package (VASP) framework.[3] The projector-augmented wave (PAW) method was employed to describe electron-ion interactions.[4] The Perdew-Burke-Ernzerhof (PBE) functional, known for its accuracy in simulating adsorbate systems, was used to treat exchange-correlation effects.[5] Dispersion corrections were included using the DFT-D3 method with the Becke-Johnson damping scheme.[6] A plane-wave cutoff energy of 500 eV was used throughout all calculations. Geometric optimizations were carried out until the residual forces on each atom were less than 0.01 eV $Å^{-1}$. A vacuum layer of at least 15 Å was applied to avoid interaction between periodic images. The Brillouin zone was sampled using a 3×3×1 Monkhorst-Pack k-point mesh for structural optimizations and a finer 10×10×1 mesh for electronic structure calculations.[7]

The Mo-O-Ni interface was modeled using a periodic slab model. The substrate is a Keggin-type phosphomolybdic acid (PMA) polyoxometalate, with crystal structure data taken from the Materials Project database (monoclinic, space group *C*2/c). The (001) surface of PMA was cleaved, exposing bridging oxygen atoms that form a four-fold hollow site. A Ni cluster was anchored at this four-fold hollow site, coordinating with four surface bridging oxygen atoms to create the Mo-O-Ni interface via Mo-O-Ni bridging bonds. A p(2×2) supercell was constructed with a vacuum layer of 20 Å. The bottom layer was fixed to bulk positions while the top layers and the anchored Ni cluster

were fully relaxed. The adsorption energy (Eads) was calculated using the following equation[8]:

$E_{ads} = E_{total}-E_{sub}-E_{mol}$

where E_{mol} is the energy of the isolated adsorbate molecule.

Free energy calculations were performed by including vibrational entropy contributions within the harmonic approximation.[9] The Gibbs free energy (G) at temperature T was computed as:

$G = EDFT + ZPE – TS$

where EDFT is the DFT total energy, ZPE is the zero-point energy, S is the entropy, and T is the temperature. The ZPE and entropy were calculated from the vibrational frequencies.

Reaction pathways and energy barriers were determined using the climbing-image nudged elastic band (CINEB) method.[10]

Table S1 The conversion of naphthalene and the selectivity of products obtained over a physical mixture of metallic Ni and PMA.

Catalyst	Conv. (%)	Yield / %		
		decalin	1,9-octalin	Tetralin
Ni+PMA physical mixture	69.2	0	0	69.2

Reaction conditions: 100 mg naphthalene, 50 mg catalyst, 20 mL n-hexane, 180℃, 2 MPa H_2, 4 h.

Table S2 The conversion of naphthalene and the selectivity of products over 12%-PMA@Ni at different H_2 pressure.

Entry	H_2 pressure (MPa)	Conv. (%)	Yield / %		
			decalin	1,9-octalin	Tetralin
1	0.5	99.50	45.70	0.40	53.90
2	1	99.90	97.10	0.00	2.90
3	1.5	99.90	97.40	0.00	2.60
4	2	99.90	97.80	0.00	2.20

Reaction conditions: 100 mg naphthalene, 50 mg catalyst, 20 mL n-hexane, 180℃, 4 h.

Table S3 The conversion of naphthalene and the selectivity of products over 12%-PMA@Ni at different reaction time.

Entry	Time (h)	Conv.(%)	Yield / %		
			decalin	1,9-octalin	Tetralin
1	1	98.40	13.20	1.70	85.10
2	2	99.90	97.50	0.00	2.50
3	3	99.90	97.30	0.00	2.60
4	4	99.90	97.80	0.00	2.20

Reaction conditions: 100 mg naphthalene, 50 mg catalyst, 20 mL n-hexane, 180℃, 1 MPa H_2.

Table S4. Comparison of 12%-PMA@Ni with reported metal catalysts for naphthalene hydrogenation.

Catalyst	Temperature (°C)	Pressure (MPa)	Time (h)	Conv. (%)	Selectivity (%)	Ref.
Pd-Pt/Al_2O_3-SAPO-11	260	4	12	100	91	11
Pd5%/Al_2O_3	250	4	2	99	99.5	12
Pt/BNASA	240	4	12	100	100	13
Pt/Hβ-2	220	4	12	94.2	81.4	14
Pd/HY-9.5	200	4	1	100	73.15	15
Ni/M-Beta	200	5	3	100	100	16
Ni_2P/SiO_2	340	4	0.18	100	92.1	17
Pt/HZSM-5-25	250	5	1	99.7	65.6	18
NiMo	200	3	0.33	99.9	99.9	19
12%-PMA@Ni	180	1	2	99.9	97.5	This work

Table S5 ICP-OES results for Ni and Mo in the post-reaction solution after each cycle.

Entry	Ni	Mo
Cycle 1 leachate	2.32 μg	0.22 μg
Cycle 2 leachate	2.35 μg	0.23 μg
Cycle 3 leachate	2.27 μg	0.22 μg
Cycle 4 leachate	4.38 μg	0.49 μg

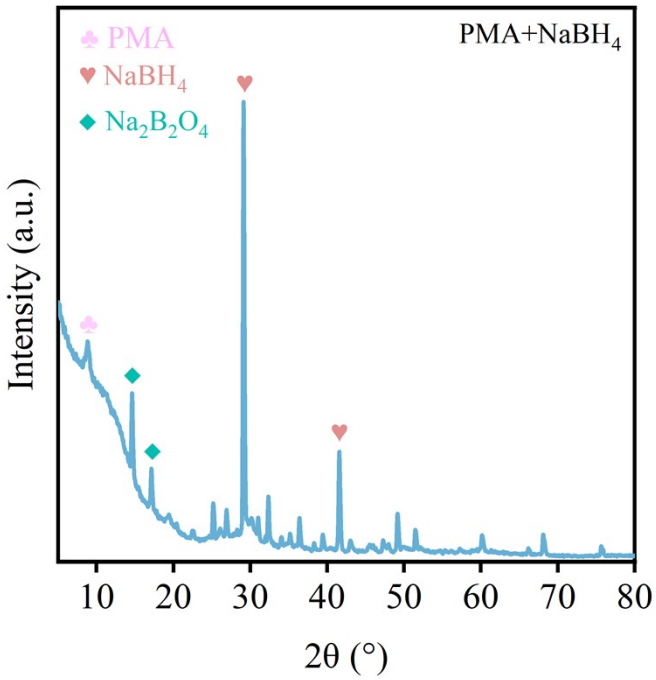

Figure S1 XRD patterns of unwashed catalyst obtained from the reaction of PMA with $NaBH_4$.

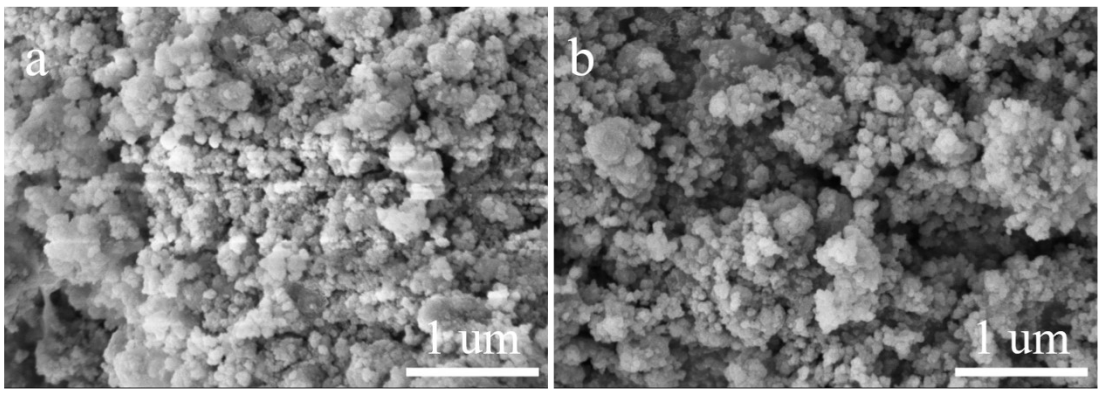

Figure S2 SEM images of (a) 6%-PMA@Ni and (b) 24%-PMA@Ni.

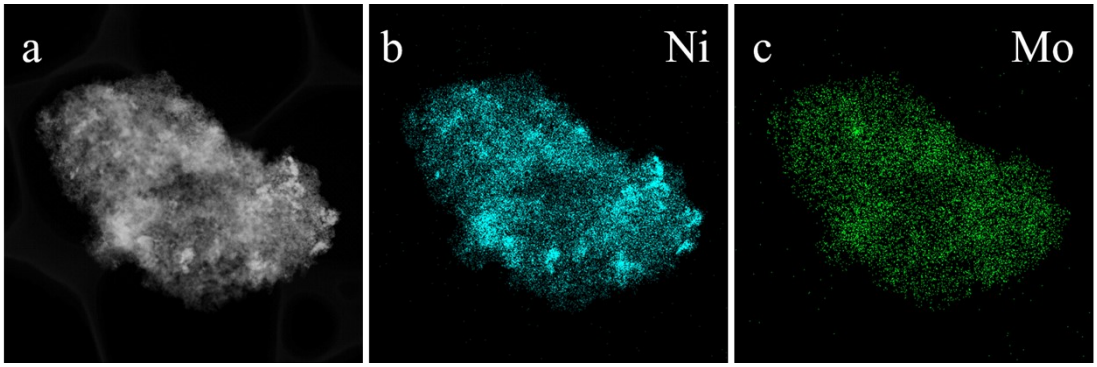

Figure S3. (a-c) Elemental mappings of 12%-PMA@Ni.

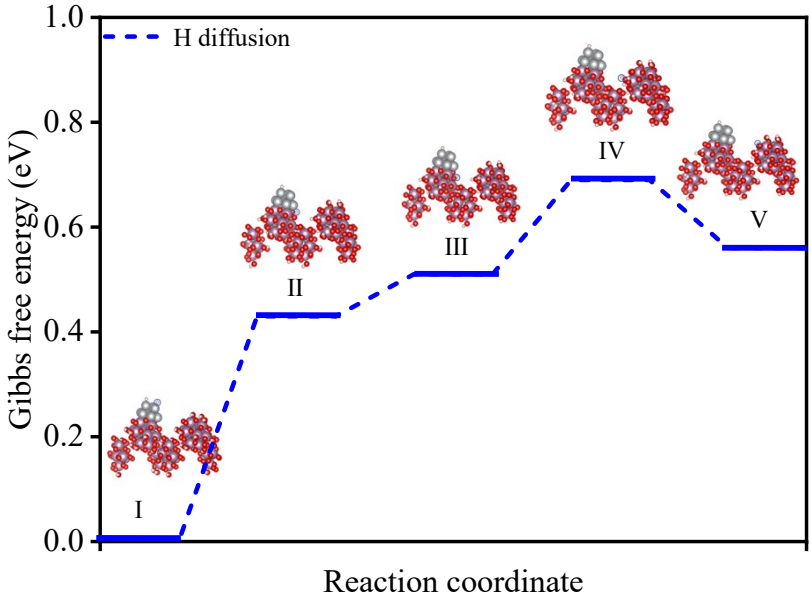

Figure S4 Free energy diagram of hydrogen spillover over 12%-PMA@Ni. Gray, purple, red, and pink spheres represent Ni, Mo, O, and H atoms, respectively.

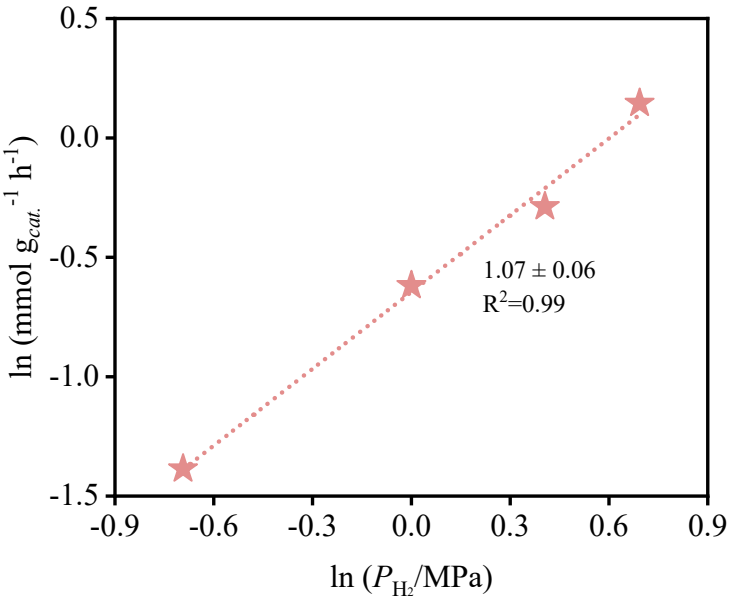

Figure S5 The conversion rate of naphthalene as a function of H_2 pressure. The conversion rate is taken in mmol g_{cat}^{-1} h^{-1} units for calculations. Reaction conditions: 90 °C, 2 h, 100 mg naphthalene, 50 mg catalyst, 20 mL n-hexane.

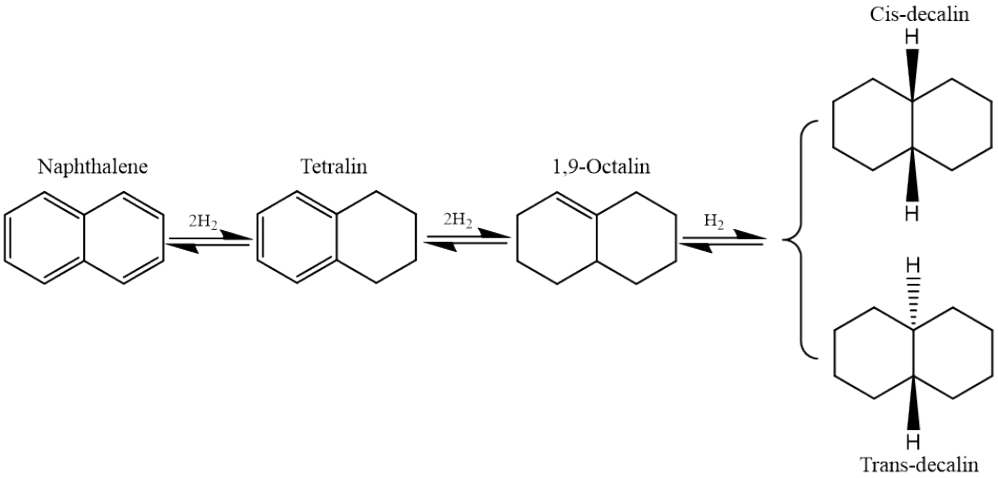

Figure S6 Proposed reaction mechanism for the hydrogenation of naphthalene over 12%-PMA@Ni.

References

1. X. R. Ye, D. Z. Jia, J. Q. Yu, X. Q. Xin and Z. Xue, *Adv. Mater.*, 1999, **11**, 941–942.

2. J. Wang, Y. Tang, X. Guo, L. Liu, Y. Zhang, T. Liu, J. Liu, X. Zhou, X. Li and D. Jia, *Inorg. Chem.*, 2025, **64**, 12409–12415.

3. G. Kresse and J. Furthmüller, *Phys. Rev. B*, 1996, **54**, 11169–11186.

4. P. E. Blöchl, *Phy. Rev. B*, 1994, **50**, 17953–17979.

5. J. P. Perdew, K. Burke and M. Ernzerhof, *Phys. Rev. Lett.*, 1996, **77**, 3865–3868.

6. S. Grimme, J. Antony, S. Ehrlich and H. Krieg, *J. Chem. Phys.*, 2010, **132**,154104.

7. H. J. Monkhorst and J. D. Pack, *Phys. Rev. B*, 1976, **13**, 5188–5192.

8. M. A. Johnson, *Nat. Chem.*, 2009, **1**, 8–9.

9. G. Kresse and J. Furthmüller, *Comput. Mater. Sci.*, 1996, **6**, 15–50.

10. G. Henkelman and H. Jónsson, *J. Chem. Phys.*, 2000, **113**, 9978–9985.

11. M. Du, Z. Qin, H. Ge, X. Li, Z. Lü and J. Wang, *Fuel Process. Technol.*, 2010, **91**, 1655–1661.

12. R. M. Claydon, L. A. Roman-Ramirez and J. Wood, *ACS Omega*, 2021, **6**, 20053–20067.

13. D. Li, Z. Liu, L. Qiao, X. Kong, E. Wang, H. Li, L. Jin, C. Wang, C. Xu and X. Wang, *J. Catal.*, 2025, **452**.

14. Z. Liu, J. Mei, D. Wang, X. Kong, K. Yu, Z. Cao, C. Wang, Y. Gong, A. Duan, C. Xu and X. Wang, *Fuel*, 2024, **368**.

15. M. Zhang, Q. Song, Z. He, Q. Wang, L. Wang, X. Zhang and G. Li, *Int. J.*

Hydrogen Energy, 2022, **47**, 20881–20893.

16. X. Zhang, K. Meng, H. Liu, B. W. Biney, Y. Qi, K. Xu, J. Wu, L. Xie, X. Li, Y. Liu, K. Chen, Z. Wang and A. Guo, *J. Energy Chem.*, 2025, **106**, 1026–1037.

17. X. Zhang, Q. Zhang, A. Zhao, J. Guan, D. He, H. Hu and C. Liang, *Energy Fuels*, 2010, **24**, 3796–3803.

18. J. Liu, H. Zhang, N. Lu, X. Yan, B. Fan and R. Li, *Ind. Eng. Chem. Res.*, 2020, **59**, 1056–1064.

19. H. Liu, C. Liu, C. Yin, B. Liu, X. Li, Y. Li, Y. Chai and Y. Liu, *Catal. Today*, 2016, **276**, 46–54.